



SEISMIC HAZARD IN WESTERN CANADA FROM GLOBAL POSITIONING SYSTEM STRAIN RATE DATA

L. J. Leonard¹, S. Mazzotti², J. C. Cassidy², G. Rogers², and S. Halchuk³

ABSTRACT

Probabilistic seismic hazard analyses are principally based on frequency-magnitude statistics of historical and instrumental earthquake catalogues. This method assumes that return periods of large damaging earthquakes (100s–1000s yr) can be extrapolated from 50-100 yr statistics of small and medium earthquakes. The method has obvious limitations when applied to areas of low-level seismicity where the earthquake statistics may be poorly constrained. In this study, we test an alternative approach to assess seismic hazard in Western Canada. We use horizontal velocities at ~250 Global Positioning System (GPS) sites in BC and Alberta to calculate strain rates and earthquake statistics within seismic source zones. GPS-based strain rates are converted to seismic moment, earthquake frequency-magnitude statistics, and seismic hazard using a logic-tree method. The GPS-based earthquake statistics and seismic hazard are then compared to those derived from the earthquake catalogue. In one zone (Puget Sound), the GPS seismic hazard estimates are in good agreement with those from earthquake statistics. In nearly all other zones (e.g., most of BC and Alberta), the GPS seismic hazard estimates are significantly larger than those from the earthquake catalogue by one or two orders of magnitude. This discrepancy could indicate that the earthquake catalogue significantly under predicts long-term seismic hazard (over 100s–1000s yr) in areas of low-level seismicity. Alternatively, significant aseismic deformation may occur over long time-scales, which would imply that the GPS strain rates over predict the true seismic hazard. We discuss the nature and limitations of both methods in light of our results for Western Canada, with the goal of defining a methodology to incorporate GPS strain rate data into probabilistic seismic hazard assessments.

¹Postdoctoral Fellow, Geological Survey of Canada, Natural Resources Canada, 9860 W. Saanich Road, Sidney, BC V8L 4B2, Canada

²Research Scientist, Geological Survey of Canada, Natural Resources Canada, 9860 W. Saanich Road, Sidney, BC V8L 4B2, Canada

³Seismologist, Geological Survey of Canada, Natural Resources Canada, 7 Observatory Crescent, Ottawa, ON K1A 0Y3, Canada

Introduction

Probabilistic seismic hazard analyses are generally based on earthquake statistics from the historical earthquake catalogue. Typically, one assumes that, within a particular seismic zone, the frequency of infrequent large events can be predicted from the frequency-magnitude relationship of more frequent smaller earthquakes. However, there may be insufficient historical seismicity within a zone to calculate accurate earthquake statistics, i.e., the return periods of larger earthquakes are often significantly longer than the historic seismic record.

Geodetic, and particularly Global Positioning System (GPS), data have the potential to provide additional constraints on long-term seismic hazard (e.g., Ward 1998a, 1998b). After correction for transient elastic strain (e.g., interseismic strain accumulation on a subduction fault), relative motions between GPS sites allow for a good approximation of the steady-state long-term crustal strain. Such long-term crustal strain provides a maximum estimate of potential seismic hazard, as it includes both seismic and any possible aseismic processes. Thus, in cases where the GPS strain is a close match with the seismic strain, the earthquake catalogue likely provides a good estimate of the true long-term seismic hazard. Conversely, where GPS data point to significantly greater long-term strain than implied by earthquake data, the earthquake catalogue may considerably under predict the long-term seismic hazard. However, some caution is necessary in the interpretation of both datasets due to their inherent assumptions and uncertainties. If significant aseismic processes occur, GPS estimates of long-term strain will over predict the actual seismic hazard. Also, the choice of zone boundaries, and the distribution of GPS stations within them, can have a significant impact on the results.

In this paper, we use GPS horizontal velocity data from about 250 sites as an alternative dataset to estimate seismic hazard in Western Canada, independent of the earthquake catalogue. Assuming a direct relationship between crustal deformation and seismicity, we estimate current crustal strain rates, equivalent seismic moment, earthquake statistics, and seismic hazard within a number of seismic source zones (Fig. 1) from the seismically active west coast to the more stable plains of Alberta. The GPS-derived earthquake statistics and seismic hazard are then compared with those based on the earthquake catalogue.

Methodology

Earthquake Data

The earthquake catalogue (Figure 1) is treated to remove plate boundary and oceanic slab events from zones 6 to 11, and industry-induced events from zones 1 to 3, so that the remaining seismicity is related purely to crustal deformation of the North America plate. It is also treated for completeness (for each zone only those events that match or exceed the limits of complete detection for each time period are used), using the magnitude intervals of completeness from the fourth generation seismic hazard maps of Canada (Adams and Halchuk 2003). We use a maximum likelihood method to calculate a - and b -values from the seismicity within each zone (Adams and Halchuk 2003). In zones with little seismicity (e.g., only 9 and 12 events meet the completeness limits for zones 5 and 7, respectively), these values should be treated with caution.

The a - and b -values define magnitude-frequency relationships, assuming that the seismicity follows a Gutenberg-Richter relation truncated asymptotically at an assumed maximum magnitude M_x . We choose values of M_x adapted from those given in Adams and Halchuk (2003), i.e., 7.5 ± 0.3 for the coastal zones (6-11) and 7.0 ± 0.5 for the other zones (1-4, 12).

GPS Data

The GPS dataset (Figure 2) includes horizontal velocity vectors from about 250 continuous and campaign sites throughout western Canada and extending into northwestern U.S. (cf. Mazzotti et al. 2008). The GPS data are first corrected for plate-boundary interseismic motion using geodetically- and thermally-constrained models for the Cascadia subduction zone (Wang et al. 2003) and the Queen Charlotte fault (both strike- and dip-slip components, Mazzotti et al. 2003).

Within each zone, we use a least-square inversion to derive a homogeneous strain rate tensor, rigid translation, and rigid rotation model from the horizontal GPS velocities. For zones with few (≤ 4) GPS sites (e.g., zones 3 and 5), we use additional nearby data points from neighboring zones to better constrain the strain rate inversion. The strain rate tensor is resolved into its two principal components ε_1 and ε_2 (both magnitude and azimuth) and their relative uncertainties (negative values indicate shortening). The resolved GPS-derived strain rate components for each zone are shown in Figure 3, along with estimated rates of block translation and rotation.

Using a logic-tree method to incorporate parameter uncertainties (e.g., Mazzotti et al. 2005), we then calculate the equivalent seismic moment rate, M_0' , that would occur if the strain is entirely seismic, using the following equation (Savage and Simpson 1997):

$$M_0' = 2 \mu h A \text{Max}(|\varepsilon_1|, |\varepsilon_2|, |\varepsilon_1 + \varepsilon_2|) \quad (1)$$

where μ is the shear modulus (3.0×10^{10} N/m² for crustal rocks, Turcotte and Schubert 2002), h is the effective seismic thickness, and A is the area of the zone. Assuming a b -value of 0.9 ± 0.05 , and values of M_x as given above, we calculate the a -values matching M_0' derived from the strain analysis of GPS data (cf. methodology in Mazzotti et al. 2005) to generate frequency-magnitude statistics for comparison with those generated directly from the GSC earthquake catalogue (Fig. 4).

Seismic Hazard

Comparisons between the GPS- and earthquake-derived earthquake statistics indicate that there is fair agreement between earthquake and GPS data in only one of the twelve zones considered: zone 11 - the inner Cascadia forearc of Puget Sound and the southern Strait of Georgia (Fig. 4). All other zones show a large discrepancy between the GPS- and earthquake-derived statistics, with frequency-magnitude statistics and seismic moment rates estimated from GPS typically one to two orders of magnitude higher than the earthquake-based rates (e.g., zone 1, Fig. 4). Using a different methodology, Ward (1998a, 1998b) found a similar bias towards

significantly higher geodetic strain rates, compared to earthquake catalogue strain rates, in regions of the U.S.A. and Europe. In contrast, agreement between geodetic and seismic rates (as for our zone 11) has been documented in specific cases (e.g., Mazzotti et al. 2005, Pancha et al. 2006).

Ground shaking probabilities are not linearly related to strain and seismic moment rates, so the implications for seismic hazard must be examined separately. We use the GSCFRISK seismic hazard code (e.g., Adams and Halchuk 2003) to evaluate ground shaking probabilities from crustal earthquakes using the GPS-based and earthquake-based source models independently. For each model, we estimate spectral and peak ground accelerations at various standard probabilities (not shown here). As an example, Figure 5 shows the ratio of GPS-based over earthquake-based spectral acceleration at 1.0 second for 2% probability of exceedance in 50 years; note that the resultant map does not show seismic hazard, but rather the ratio of the output from the two methods. In this example, the spectral acceleration in zone 11 (the zone with closest agreement in strain rates) is 1.5 times greater from the GPS model than the earthquake model. In most other zones, spectral accelerations are 3 to 4 times greater in the GPS model. In zones 1 and 5, where strain estimated from the earthquake catalogue is essentially near-zero, the GPS model predicts spectral accelerations that are 9 to 10 times greater than the earthquake model.

As mentioned above, the greater strain indicated by the GPS data relative to the earthquake data could indicate that the earthquake-derived seismic hazard is significantly underestimated in much of western Canada. However, other reasons for the discrepancy must be considered, that would conversely imply overestimation of seismic hazard from GPS data. Possible explanations include aseismic deformation and block rotations mapped in GPS strain rates, which would not result in seismic deformation. Significant aseismic deformation may occur as creep on faults (such as the southern section of the San Andreas Fault, e.g., Moore and Rymer 2007). Large-scale block rotations could explain some of the apparent strain (such as clockwise rotation of the Oregon block, McCaffrey et al. 2007), but there should still be deformation occurring at the edges of such blocks (such as leading-edge shortening in relation to the Oregon block rotation). A possible candidate for aseismic deformation is the apparent distributed right-lateral shear occurring between the Queen Charlotte Islands and the inland areas to the east (zone 6 to zone 5; Figure 2). These motions could also be the result of clockwise rotation of a quasi-rigid block, with extension at its trailing edge to the south (as suggested by the GPS-derived principal strains in northern Cascadia (zone 7; Figure 3), and compression expected at its leading edge to the north/northeast.

Conclusions

We tested an alternative approach to assess seismic hazard in Western Canada using GPS strain rate data to derive earthquake statistics, seismic moment and ground shaking probabilities in seismic source zones. In one zone (Puget Sound), the GPS-based seismic hazard estimates are in agreement with the earthquake-based ones. In all other zones, the GPS-based seismic hazard estimates are one or two orders of magnitude larger than the earthquake-based ones.

Explanations for this discrepancy may be that the earthquake catalogue significantly under predicts true seismic hazard, or alternatively that GPS over predicts true hazard due to significant aseismic deformation. GPS-based strain rates and earthquake statistics can provide an important and useful complement for seismic hazard analysis, but significant research is still required to better understand the limitations and applicability of this new method.

Acknowledgments

We thank John Adams and Roy Hyndman for numerous discussions and help with this project. GSC Contribution #XXXXXXXX.

References

- Adams, J., and S. Halchuk, 2003. Fourth generation seismic hazard maps of Canada: values for over 650 Canadian localities intended for the 2005 National Building Code of Canada, *Geological Survey of Canada Open File 4459*, 155 p.
- Mazzotti, S., R. D. Hyndman, P. Flück, A. J. Smith, and M. Schmidt, 2003, Distribution of the Pacific-North America motion in the Queen Charlotte Islands-S. Alaska plate boundary zone, *Geophysical Research Letters*, 30, 1762, doi:10.1029/2003GL017586.
- Mazzotti, S., T. S. James, J. Henton, and J. Adams, 2005, GPS crustal strain, postglacial rebound, and seismicity in eastern North America: The St Lawrence valley example, *Journal Geophysical of Research*, 110, B11301, doi:10.1029/2004JB003590.
- Mazzotti, S., L. J. Leonard, R. D. Hyndman, and J. F. Cassidy, 2008, Tectonics, Dynamics, and Seismic Hazard in the Canada-Alaska Cordillera, in Freymueller, J. T., P. J. Haeussler, R. L. Wesson, and G. Ekstrom, eds., *Active Tectonics and Seismic Potential of Alaska: Geophysical Monograph Series*, 179, p. 297-319, American Geophysical Union.
- McCaffrey, R., A.I. Qamar, R.W. King, R. Wells, G. Khazaradze, C.A. Williams, C.W. Stevens, J.J. Vollick, and P.C. Zwick, 2007. Fault locking, block rotation and crustal deformation in the Pacific Northwest, *Geophysical Journal International*, 169, doi:10.1111/j.1365-246X.2007.03371.x.
- Moore, D. E., and M. J. Rymer, 2007. Talc-bearing serpentinite and the creeping section of the San Andreas fault, *Nature*, 448, 795–797, doi:10.1038/nature06064.
- Pancha, A., J. G. Anderson, and C. Kreemer, 2006, Comparison of seismic and geodetic scalar moment rates across the Basin and Range Province, *Bulletin of the Seismological society of America*, 96, 11-32.
- Savage, J.C. and R.W. Simpson, 1997. Surface strain accumulation and the seismic moment tensor, *Bulletin of the Seismological Society of America*, 87 (5), 1345-1353.
- Turcotte, D.L., and G. Schubert, 2002. *Geodynamics*, Cambridge University Press, Cambridge, UK, 456

p.

Wang, K., R. Wells, S. Mazzotti, R.D. Hyndman, and T. Sagiya, 2003. A revised dislocation model of interseismic deformation of the Cascadia subduction zone, *Journal of Geophysical Research*, 108 (B1), doi: 10.1029/2001JB001227.

Ward, S. N., 1998a, On the consistency of earthquake moment release and space geodetic strain rates: United States, *Geophysical Journal International*, 134, 172-186.

Ward, S. N., 1998b, On the consistency of earthquake moment release and space geodetic strain rates: Europe, *Geophysical Journal International*, 135, 1011-1018.

Figures

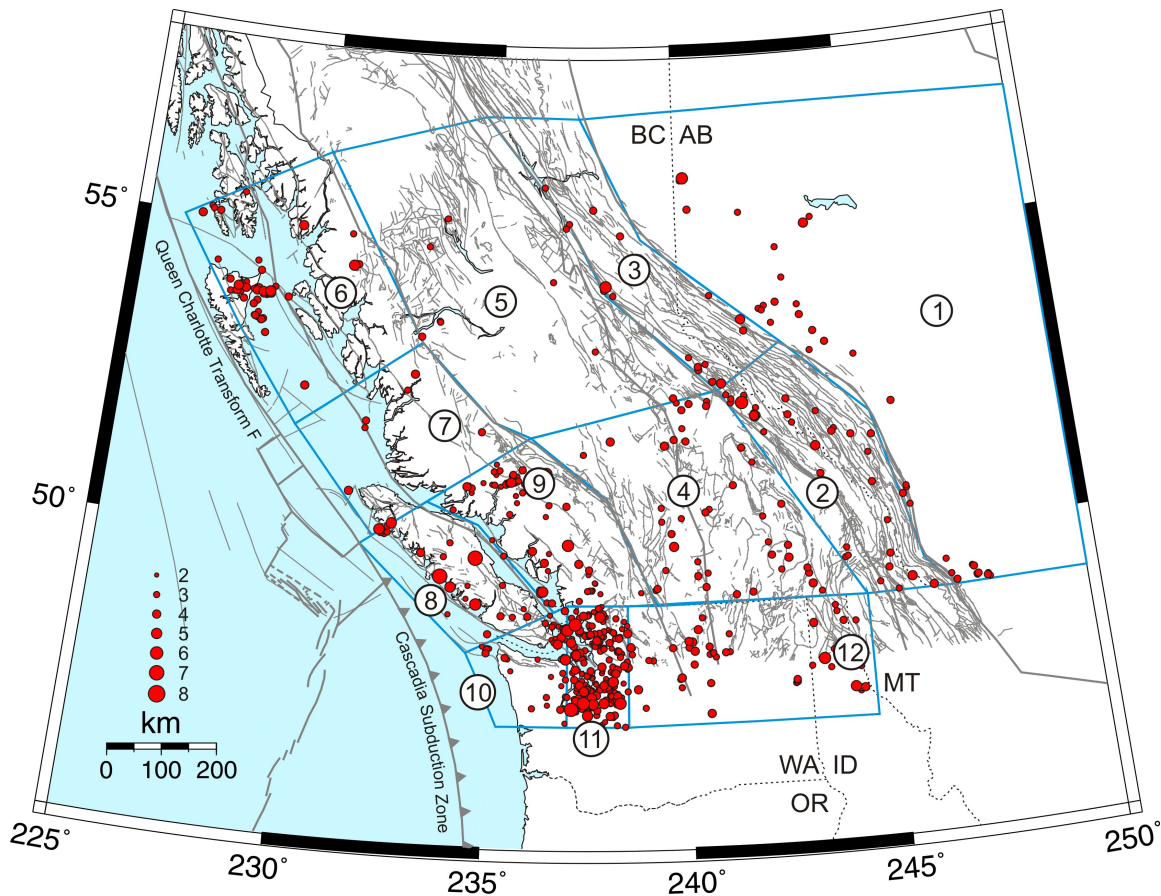


Figure 1. Crustal earthquakes in zones 1 to 12 from the GSC earthquake catalogue, 1899-2007 (red circles, scaled by magnitude). Omitted are: plate-boundary events, induced events, and earthquakes that do not meet the completeness requirements of each zone. Mapped faults are shown in grey. Seismic zone boundaries are shown in blue.

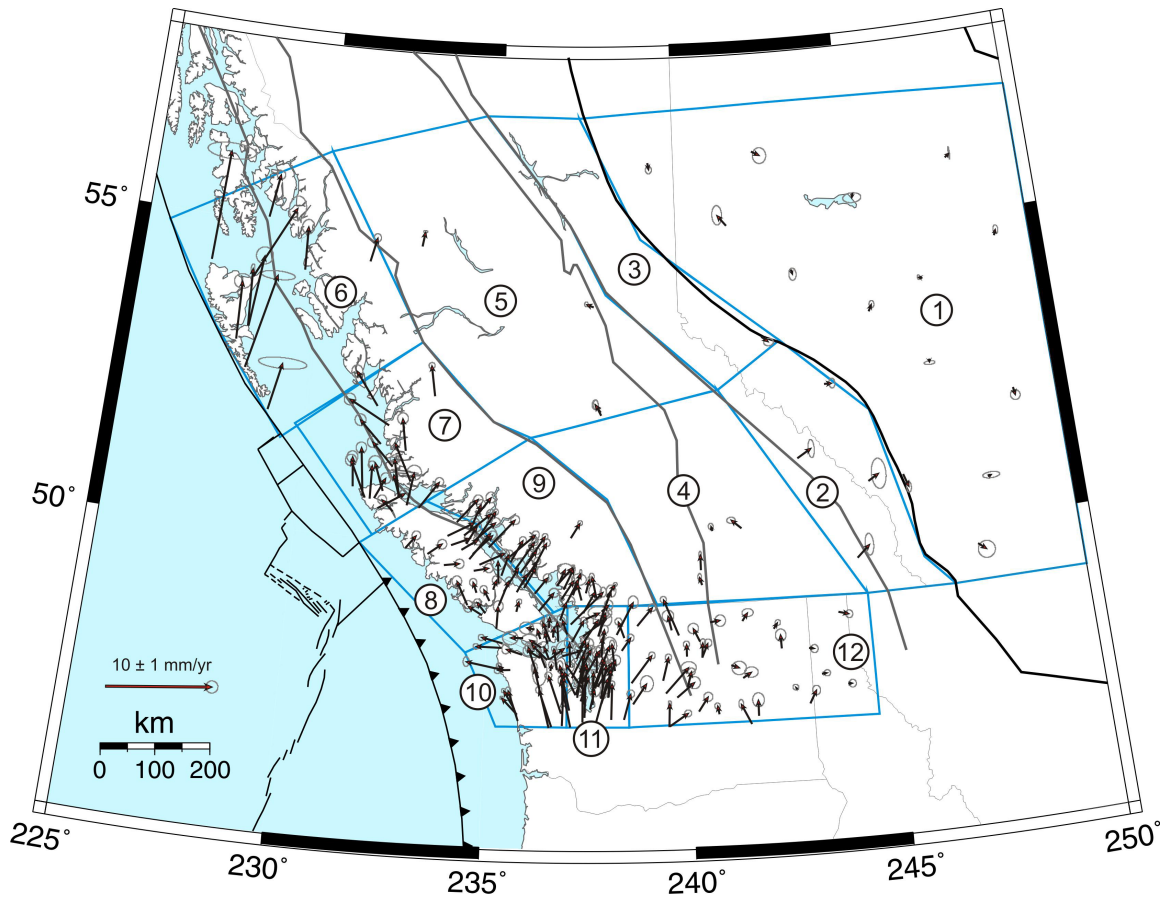


Figure 2. GPS residual velocity vectors (black arrows) relative to stable North America (in ITRF2000), after correction for interseismic strain accumulation on the western N. America plate boundary faults (dip slip on the Cascadia subduction fault; strike- and dip-slip on the Queen Charlotte fault). Ellipses show the 66% confidence intervals.

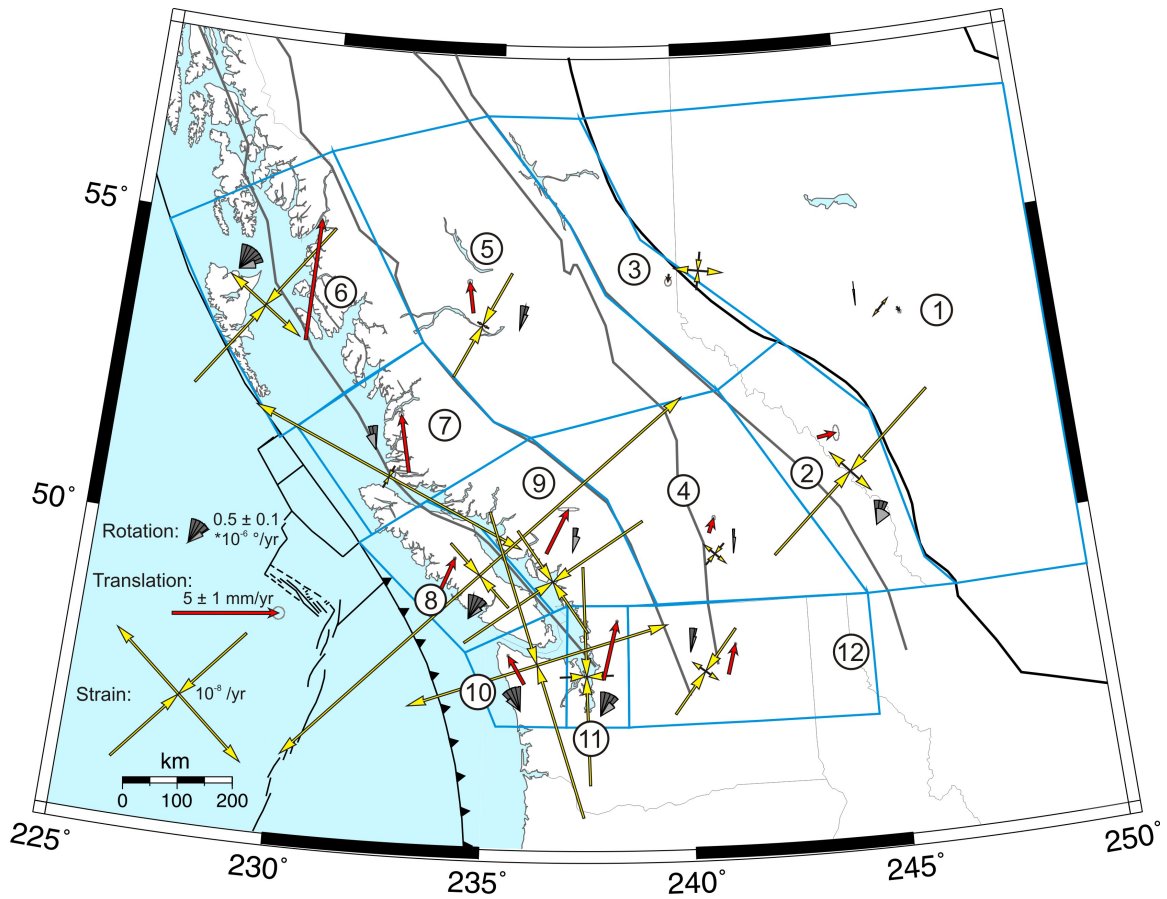


Figure 3. Principal horizontal components of strain (yellow arrows), translation (red vectors), and rotation (grey wedges) rates resolved from GPS data, assuming uniform strain, translation, and rotation within each zone.

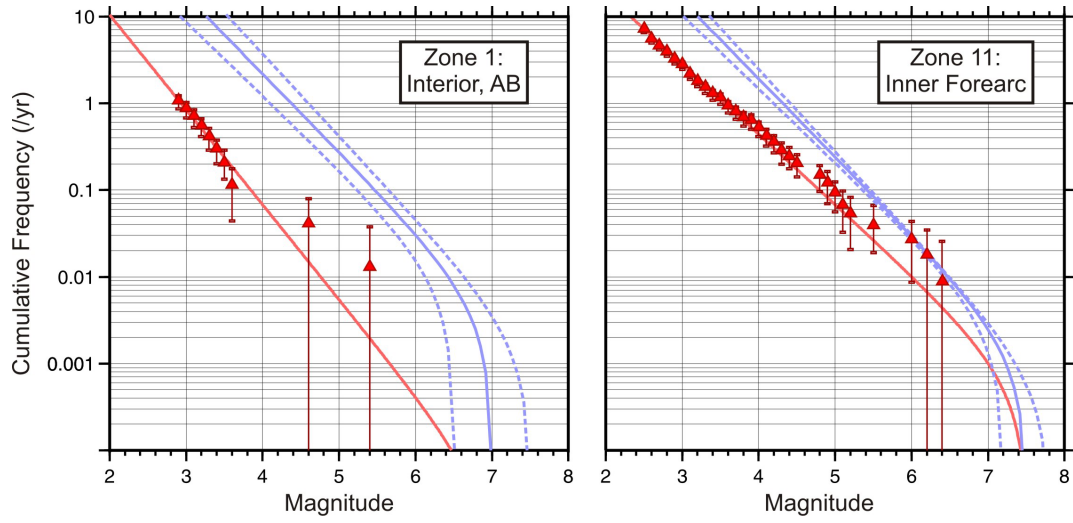


Figure 4. Comparison of earthquake recurrence statistics for zones 1 - Interior (left) and 11 - Inner Forearc (right). Cumulative frequency distributions from earthquake catalogue data (red triangles and maximum-likelihood best fit line) and from GPS strain rate data (blue lines show median and 66% confidence region).

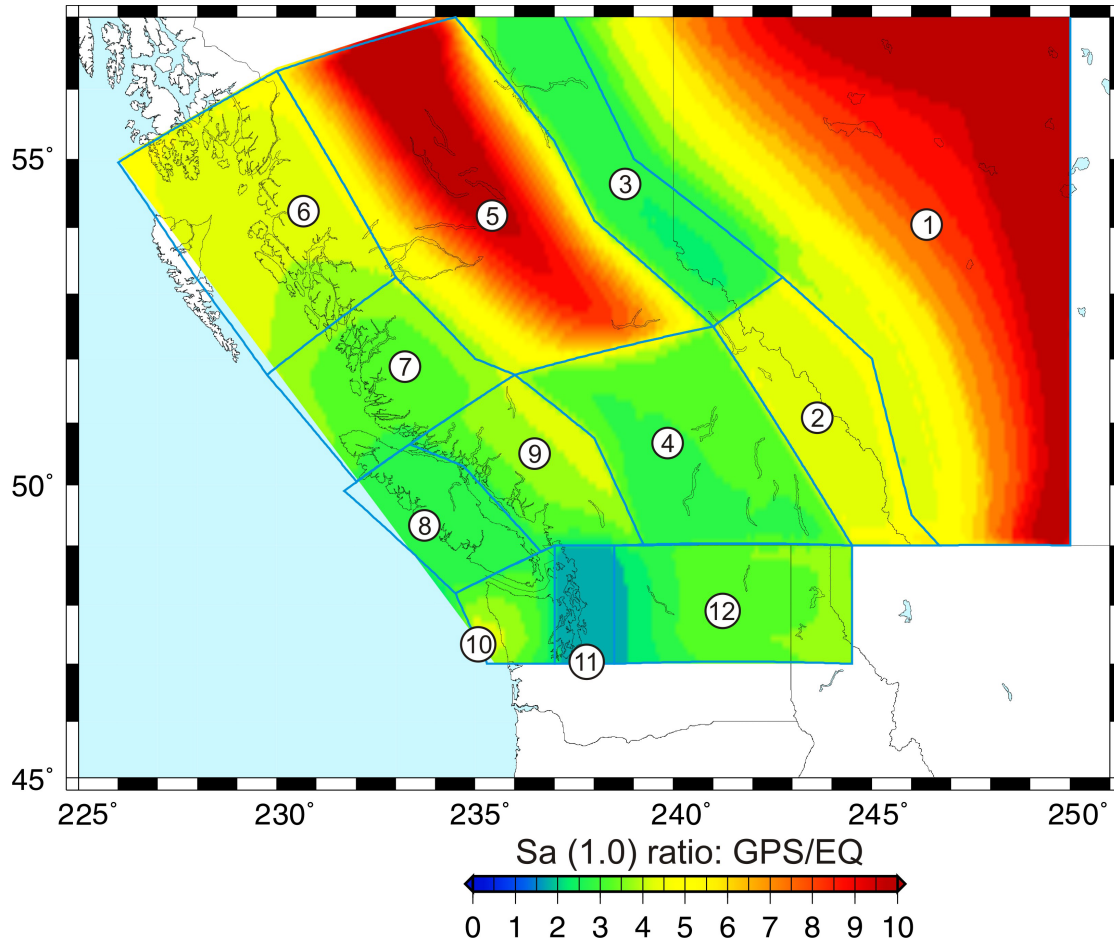


Figure 5. Ratio of ground shaking probability derived from GPS strain rates vs. earthquake catalogue. The ratio is shown for spectral acceleration at 1.0 seconds for a 2% probability of exceedance in 50 years. E.g., in zone 11, $Sa(1.0)$ from GPS data is ~ 1.5 times larger than that from the earthquake catalogue. N.B. this is a comparative map, not a seismic hazard map.